J Solid State Electrochem (2010) 14:1649–1656
DOI 10.1007/s10008-009-0998-8

ORIGINAL PAPER

Enhanced ionic conductivity in novel nanocomposite gel polymer electrolyte based on intercalation of PMMA into layered LiV_3O_8

Madhuryya Deka · Ashok Kumar

Received: 28 July 2009 / Revised: 21 December 2009 / Accepted: 27 December 2009 / Published online: 4 February 2010

Abstract In the present work, a novel polymer electrolyte based on poly(methyl methacrylate) (PMMA)/layered lithium trivanadate (LiV_3O_8) nanocomposite has been investigated. X-ray diffraction (XRD) study shows that d-spacing is increased from 6.3±0.1 Å to 12.8±0.1 Å upon intercalation of the polymer into the layered LiV_3O_8. Room temperature ionic conductivity of the obtained nanocomposite gel polymer electrolyte is found to be superior to that of conventional PMMA-based gel polymer electrolyte. Enhancement in ionic conductivity of the nanocomposite gel electrolyte is attributed to the formation of a two-dimensional channel as a result of decreased interaction between Li^+ and $V_3O_8^-$ layers as confirmed by FTIR. SEM results show aggregation of nanocomposite particles resulting from extension of some of the polymer chains from interlayer to the edge providing paths for Li^+ ion transport. Interfacial stability of nanocomposite gel electrolyte is also found to be better than that of the conventional PMMA-based gel polymer electrolyte.

Keywords Layered compounds · Polymers · Impedance spectroscopy · Ionic conductivity · Intercalation

Introduction

The development of new polymer electrolytes has been an important research area in the last three decades for applications in various electrochemical devices particularly in solid-state rechargeable lithium batteries [1]. Compared with the liquid electrolytes, polymer electrolytes offer flexibility and shape versatility, which provides a compelling rationale to use them in rechargeable lithium batteries. However, the archetypal PEO-based polymer electrolytes offer poor ionic conductivity (10^{-8} S cm^{-1}) at room temperature, which excludes them from practical applications [2]. In order to enhance the room temperature ionic conductivity of the polymer electrolytes several strategies have been developed that include incorporating organic solvents (plasticizers) to form plasticized or gel polymer electrolytes [3–5], doping with inorganic fillers to make composite polymer electrolytes [6] and synthesizing new polymers [7]. A common approach is to allow the polymer network to swell in presence of solvents or plasticizers such as ethylene carbonate, propylene carbonate (PC), diethyl carbonate (DEC), etc. to develop polymer gel electrolytes. Due to the presence of the solvent, the overall ionic conductivity reflects the conductivity of the solvent(s) rather than that of the solid polymer electrolytes [8]. These gelled or plasticized polymer electrolytes can exhibit ionic conductivity as high as 10^{-3} S cm^{-1} [8]. One of the gel polymer electrolytes, that have been extensively investigated, is that containing poly(methyl methacrylate) (PMMA) [9–13]. However, reasonable conductivity achieved using such plasticized film is offset by poor mechanical properties at high plasticizer content. Rajendran et al. [14, 15] reported the improvement in the mechanical properties of PMMA by blending with poly(vinyl alcohol) (PVA). However, a decrease in ionic conductivity was observed at higher PVA content due to increased viscosity. The increase in viscosity at higher PVA content is ascribed to the polymer-solution interaction, which decreases the ionic mobility resulting in decreased ionic conductivity [15]. On the other hand nano-

M. Deka · A. Kumar (✉)
Materials Research Laboratory, Department of Physics,
Tezpur University,
Napaam,
Tezpur 784028, India
e-mail: ask@tezu.ernet.in

composite gel polymer electrolytes based on addition of nanosized ceramic fillers has proved to give high ionic conductivity coupled with better electrochemical and interfacial stability [16, 17]. The addition of inorganic fillers can prevent the polymer chain reorganization, which promotes the ion transportation and improves the interfacial and electrochemical stability.

Polymers intercalated into low-dimensional host lattices form an attractive class of compounds [18], since intercalation can combine properties of both the guest polymer and the inorganic host in a single material. These compounds also serve as model systems for understanding the effect of confinement on properties of the guest in relation to those in bulks [19, 20]. These are known as "intercalation nanocomposites". Many recent studies reveal that intercalation of ion conducting polymers into layered materials such as montmorillonite (ε=3.81), hectorite (ε=2.95), etc. can lead to the improvement of properties in terms of ionic conductivity and other electrochemical performances [21–23]. In most studies, intercalation of polymer chains in the galleries of layered materials appears to suppress their tendency to crystallize, resulting in higher ionic conductivity.

Layered lithium trivanadate (LiV_3O_8) is an inorganic material having structure of VO_6 octahedrons and VO_5 trigonal bipyramids, with the lithium ions arranged between octahedral sites [24]. This material is generally used as cathode in rechargeable lithium batteries, which shows significant electronic conductivity. However, it has been reported that upon intercalation of non-conducting polymers in these kinds of materials leads to decrease in electrical conductivity due to the increase in spatial separation of the conductive layers which increases the barrier for electron transport through the material [25, 26]. Intercalating polymer in the layered host can produce a polymer nanocomposite electrolyte with huge interfacial area. A higher interfacial area not only sustains the mechanical properties of PMMA-based gel polymer electrolytes but also increases the solubility of lithium salts due to higher dielectric property [21]

To the best of our knowledge, this work reports for the first time on the ion conducting behavior and interfacial stability of nanocomposite gel polymer electrolytes based on PMMA, LiV_3O_8, PC, DEC, and salt $LiClO_4$.

Experimental

Layered lithium trivanadate (LiV_3O_8) was prepared via solid-state reaction. The starting material LiV_3O_8 was prepared via a solid-state reaction of lithium hydroxide monohydrate ($LiOH.H_2O$, E-merck) and vanadium pentoxide (V_2O_5, E-merck). Stoichiometric $LiOH.H_2O$ and V_2O_5 (atomic molar ratio Li/V=1:5) were mixed and finely ground in an agate mortar. The mixture was then heated at 500 °C in air for 16 h as previously described [27]. 0.5 gm of PMMA (M_w= 15,000, Aldrich) was completely dissolved in 50 ml of acetone and 2 g of LiV_3O_8 was dissolved in 80 ml of ethanol. Both the solutions were mixed, stirred at 60 °C for 3 h, and then the mixed slurry was sealed in a Teflon-lined stainless steel autoclave at 100 °C for 1 d. The precipitate thus produced was filtered, washed with de-ionized water, and finally dried under vacuum at room temperature. The final powdered sample thus obtained was pressed to obtain a pellet at a pressure of 50 MPa.

The nanocomposite gel polymer electrolyte was prepared by immersing the pellet into a liquid electrolyte solution containing 1 M $LiClO_4$ in PC/DEC=1:1 (*v*/*v*), for a period of 20 h. The pellet swells quickly, and the percentage of solution uptake was calculated by the relation

$$\text{Uptake}(\%) = (W_t - W_0)/W_0 \times 100 \quad (1)$$

where W_t and W_0 are the weight of the wet and dry pellets respectively. The nanocomposite gel polymer electrolyte used in this study was denoted as PMMA-LiV_3O_8-(PC+DEC)-$LiClO_4$.

The ionic conductivity of the sample was determined from the complex impedance plots obtained by using a Hioki 3532-50 LCR HiTester in the frequency range 42 Hz to 5 M Hz. The electronic conductivity of LiV_3O_8 and PMMA-LiV_3O_8 were measured with Keithley 2400 LV source meter. The electronic conductivity of pure LiV_3O_8 is of the order of 10^{-4} S cm^{-1}, whereas after intercalation of PMMA the electronic conductivity was measured to be of the order of 10^{-7} S cm^{-1}. This confirms the insulating nature of the obtained composite material to use as electrolyte. X-ray diffractograms were taken by Rigaku miniflex diffractometer. Surface morphology of the composite electrolyte was studied by using scanning electron microscope (SEM; Jeol model JSM 6390 LV). FTIR was conducted using Nicolet Impact 410. The nature of the ionic conductivity after soaking with 1 M $LiClO_4$ in (PC+DEC) solution was measured by Wagner's polarization technique with nanocomposite polymer electrolyte between two silver (Ag) blocking electrodes. A fixed small dc potential (300 mV) was applied across the blocking electrodes and current passing through the cells was measured as a function of time for five hours to allow the samples to become fully polarized. The experimental values of the total current (I_T), which is the sum of ionic (I_i) and electronic (I_e) currents on immediate voltage application and saturated electronic current (I_e) give an estimate of ionic and electronic transport numbers in accordance with relation

$$t_{ion} = (I_T - I_e)/I_T \text{ and } t_{elc} = I_e/I_T \quad (2)$$

Results and discussion

X-ray diffraction analysis

Figure 1a–c shows the XRD patterns of pure LiV_3O_8, pure PMMA and PMMA-LiV_3O_8. It is observed that LiV_3O_8 exhibits (100) diffraction peak at an angle $2\theta = 14°$ (Fig. 1a) corresponding to the interlayer spacing (d_{100}) of 6.3±0.1 Å. Upon addition of PMMA, the diffraction peak of (100) plane of LiV_3O_8 shifts to lower angle side corresponding to the interlayer spacing of 12.8±0.1 Å (Fig. 1c). This suggests the successful intercalation of PMMA into the nanometric layers of LiV_3O_8 confirming the formation of nanocomposites [21]. The change in interlayer spacing can be expressed with the help of Bragg's equation

$$2d\sin\theta = n\lambda \tag{3}$$

where d is the distance between crystallographic planes, θ is half of the angle of diffraction, n is an integer and λ is the wavelength of X-ray. It is clear from Eq. 3 that with the increase of interlayer spacing the θ will decrease and the corresponding diffraction peak will shift towards the lower angle side. It is observed that the diffraction peaks of LiV_3O_8 become wider and weaker after intercalation. This widening of peaks indicates that LiV_3O_8 has been partially intercalated and exfoliated in PMMA matrix [28]. Moreover, the diffraction peaks corresponding to the planes (202) and (111) of LiV_3O_8 are completely absent in the nanocomposite. This could be attributed to the fact that the intercalation of PMMA has caused the LiV_3O_8 lattice structure to collapse and intercalated product is relatively poorly crystalline ascribed to the limited short-range order [29].

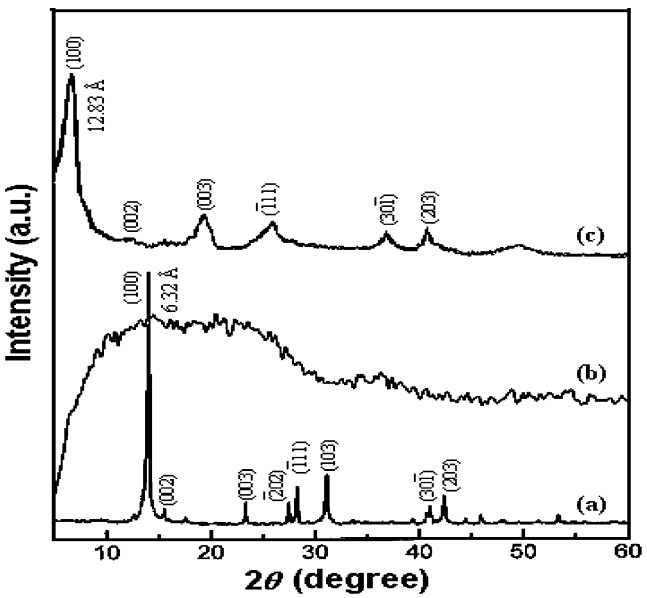

Fig. 1 X-ray diffraction patterns of **a** Pure LiV_3O_8, **b** pure PMMA and **c** PMMA-LiV_3O_8

Swelling behavior of nanocomposite

The dynamic swelling behavior of both PMMA film and PMMA-LiV_3O_8 nanocomposite pellet in 1*M* $LiClO_4$ electrolyte solution containing 1:1 (*v*/*v*) ratio of plasticizers PC and DEC at room temperature is shown in Fig. 2. It can be observed from the figure that the percent of swelling or solvent uptake for both PMMA film and PMMA-LiV_3O_8 nanocomposite pellet increases with increase in soaking period up to 11 h, but the increase in percent of swelling for nanocomposite is more as compared with that of PMMA for the same time scale. The result suggests that the solvent uptake in PMMA-LiV_3O_8 nanocomposite pellet is enhanced possibly due to the higher affinity of the layered LiV_3O_8 towards (PC+DEC)-$LiClO_4$ liquid electrolyte.

Transport number measurements

Table 1 shows the experimental values of t_{ion} and t_e for samples PMMA-(PC+DEC)-$LiClO_4$ gel polymer electrolyte and PMMA-LiV_3O_8-(PC+DEC)-$LiClO_4$ nanocomposite gel polymer electrolyte in the overall electrical transport in accordance with Eq. 2. The calculated values of ion transport number (t_{ion}) are found to be almost same (98.5%) in both the electrolytes confirming that the conductivity in both the electrolytes is essentially ionic in nature.

FTIR spectroscopy

FTIR is a powerful tool to characterize the chain structure of polymers and has led the way in interpreting the reactions of multifunctional monomers including rearrangements and isomerizations [30, 31]. FTIR spectra of pure $LiClO_4$, pure PMMA, pure LiV_3O_8, PMMA-LiV_3O_8 nanocomposite and PMMA-LiV_3O_8-(PC+DEC)-$LiClO_4$ nanocomposite gel polymer electrolyte is shown in Fig. 3a–e. The vibrational peaks of pure $LiClO_4$ are observed at 1,463 cm^{-1} and 1,087 cm^{-1} (Fig. 3a). For pure PMMA (Fig. 3b), the C=O symmetric stretch gives a sharp peak at 1,725 cm^{-1}. The peaks at 1,246 cm^{-1} and 1,151 cm^{-1} are assigned to asymmetric stretching vibration of C–O–C bond. Absorption of υ(C–O) of OCH_3 group and symmetrical stretch of C–O bond of PMMA appear at 1,187 cm^{-1} and 984 cm^{-1}, respectively [32]. The frequency 734 cm^{-1} for pure LiV_3O_8 (Fig. 3c) can be assigned to V–O–V stretching vibration, which arises because of the motion of the corner sharing oxygen atom among the VO_6, VO_5 polyhedra and Li^+ ions [33]. However the band of (V–O–V) show shifts towards lower frequency in PMMA-LiV_3O_8 nanocomposite. The shifting of peaks towards lower fre-

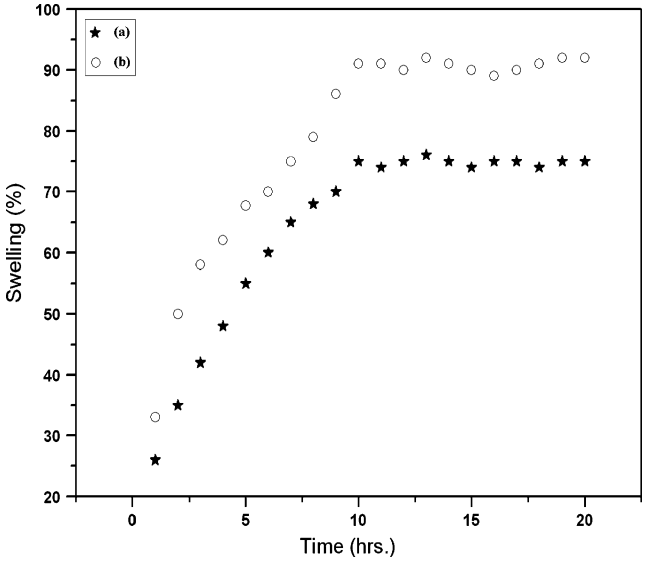

Fig. 2 Swelling behavior of **a** PMMA and **b** PMMA-LiV_3O_8 nanocomposite

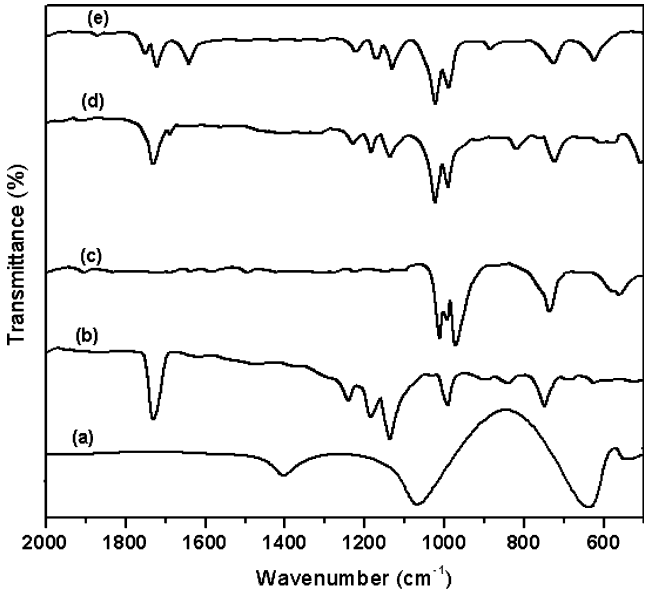

Fig. 3 FTIR spectra of **a** pure $LiClO_4$, **b** pure PMMA, **c** pure LiV_3O_8, **d** PMMA-LiV_3O_8 nanocomposite and **e** PMMA-LiV_3O_8-(PC+DEC)-$LiClO_4$ nanocomposite gel polymer electrolyte

quency in PMMA-LiV_3O_8 is a strong evidence of interaction among the lithium ions, PMMA molecules and $V_3O_8^-$ layers [34]. The bands at 990 cm^{-1}, 1,005 cm^{-1} and 972 cm^{-1} in Fig. 3c are assigned to the stretching vibration of three types of V=O groups in LiV_3O_8 crystal cell [35]. On the other hand PMMA-LiV_3O_8 nanocomposite shows only two peaks at 990 cm^{-1} and 1,025 cm^{-1} and the peak at 972 cm^{-1} disappears. This can be attributed to the decreased interaction of Li^+ ions present in the interlayer with $V_3O_8^-$ and increased interaction between Li^+ ions and PMMA molecules [33]. A small peak at 1,700 cm^{-1} appears in FTIR spectra for the nanocomposite (Fig. 3d) near the strong C=O stretching peak at 1,725 cm^{-1}, which can be ascribed to the interaction between Li^+ and the oxygen atom (a strong electron donor) of the carbonyl group of PMMA [21]. In the nanocomposite gel polymer electrolyte (Fig. 3e), frequencies 1,750 cm^{-1} and 1,644 cm^{-1} are assigned to >C=O stretching vibration of plasticizer (PC+DEC) and >C=C< bonding, respectively [36]. The $\upsilon(ClO_4^-)$ internal mode of $LiClO_4$ shows one peak at about 624 cm^{-1} which is assigned to the free anion which does not interact with lithium cation.

The assigned peaks of PMMA (1,725, 1,246, 1,187, and 1,151 cm^{-1}) are shifted to (1,710, 1,225, 1,172 and 1,143 cm^{-1}) in the nanocomposite gel polymer electrolytes. The shifting of peaks in the IR spectra suggests the interaction among the constituents of the polymer electrolyte [34].

Conductivity measurements

The Nyquist plots for LiV_3O_8, PMMA-(PC+DEC)-$LiClO_4$ and PMMA-LiV_3O_8-(PC+DEC)-$LiClO_4$ are presented in Fig. 4a–c. The impedance spectra comprise a distorted semicircular arc in the high frequency region followed by a spike in the lower frequency region [36]. The high frequency semicircle is due to the bulk properties and the low frequency spike is due to the electrolyte and electrode interfacial properties. The bulk electrical resistance value (R_b) is calculated from the intercept at high frequency side on the Z′ axis. The ionic conductivity is calculated from the relation $\sigma = l/R_b r^2 \pi$; where l and r are thickness of polymer electrolyte membrane and radius of the sample membrane discs and R_b is the bulk resistance obtained from complex impedance measurements.

The ionic conductivity value for pure LiV_3O_8 at room temperature is found to be 3.1×10^{-6} S cm^{-1} whereas for PMMA-(PC+DEC)-$LiClO_4$ electrolyte system it is 5.1×10^{-4} S cm^{-1}. This value is consistent with that reported in the literature obtained by Appetecchi et al. [37]. On the other hand, the nanocomposite gel polymer electrolyte show a maximum ionic conductivity of 1.8×10^{-3} S cm^{-1} at room temperature, which is superior to that of PMMA-(PC+

Table 1 Experimental values of ionic (t_{ion}) and electronic (t_e) transport number

Samples	Ionic transport number (%)	Electronic transport number (%)
PMMA-(PC+DEC)-$LiClO_4$	98.5	1.5
PMMA-LiV_3O_8-(PC+DEC)-$LiClO_4$	98.5	1.5

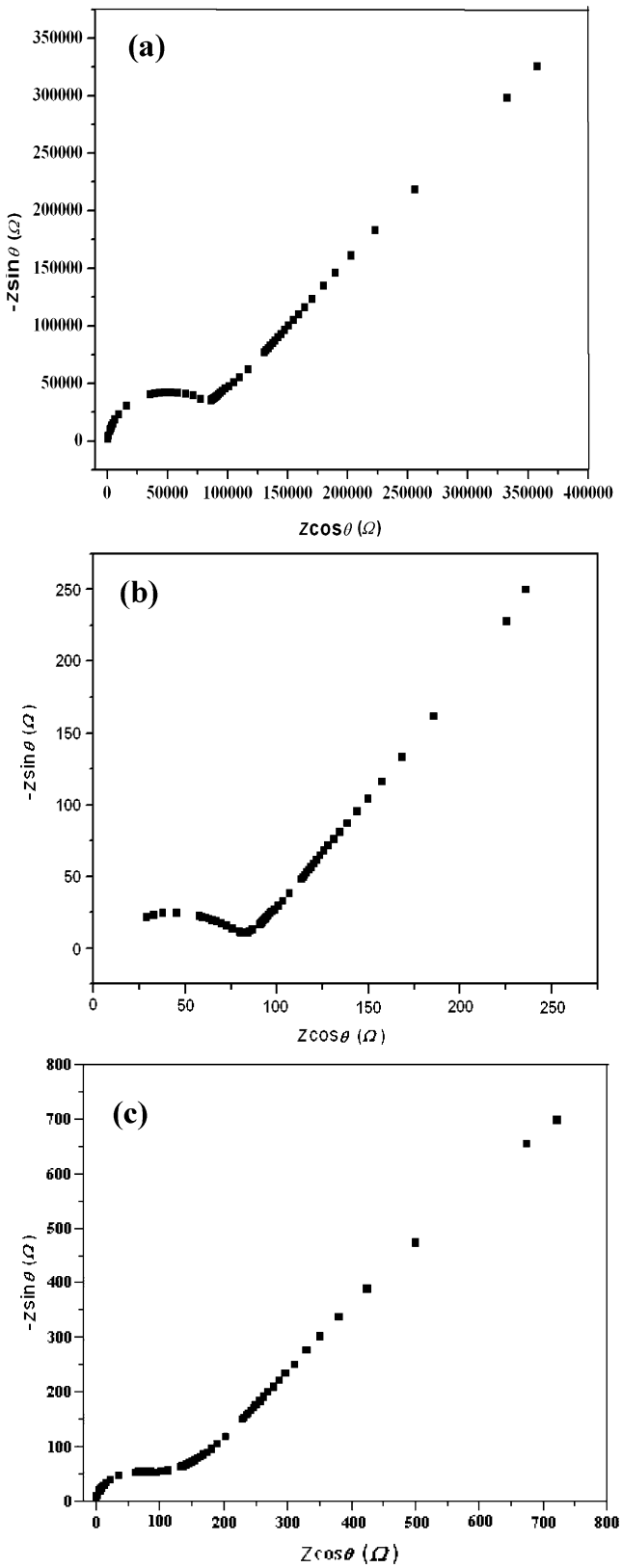

Fig. 4 Nyquist plots of **a** LiV_3O_8, **b** PMMA-(PC+DEC)-$LiClO_4$ gel polymer electrolyte and (**c**) PMMA-LiV_3O_8-(PC+DEC)-$LiClO_4$ nanocomposite gel polymer electrolyte.

DEC)-$LiClO_4$ and host material LiV_3O_8. This dramatic increase in ionic conductivity in PMMA-LiV_3O_8-(PC+DEC)-$LiClO_4$ electrolyte system is a combined result of many respects. First, it is well known that electrolytes with high dielectric constant and low viscosity can yield very high ion transport [8, 38]. In our case, the negative $V_3O_8^-$ layers in the nanocomposite with high dielectric constant (ε=4.5) could help to dissolve electrolyte salt ($LiClO_4$) more, and then increase ion conduction through the solvent domain surrounding the polymer matrix. Second, due to the extension of some polymer chains from interlayer to the edge of the nanocomposites, aggregation of nanocomposite particles takes place, which in turn provides the conduction paths for Li^+ ions to transfer between the adjacent nanocomposite grains. Third, FTIR spectra show that the interaction between lithium cations and negative $V_3O_8^-$ layers in the interlayer is weakened due to the increase in interaction between Li^+ ions and inserted PMMA molecules. This decrease in interaction between Li^+ ions and PMMA molecules may provide a two-dimensional channel for Li^+ ion transition [33]. In addition to the above, as discussed in "X-ray diffraction analysis", higher uptake of liquid electrolytes by PMMA-LiV_3O_8 nanocomposite than by PMMA may also result in higher ionic conductivity. The value of ionic conductivity obtained in this work at room temperature is better than that reported in literature for PMMA/clay systems [21, 23], where conductivity values were found to be of the order of 10^{-4}S/cm. According to the literature the residual cations present in the clay layers do not contribute to the ionic conductivity. However, the IR results described in "FTIR spectroscopy" suggest a possible strong interaction occurring between the interlayer cations and PMMA molecule and hence interlayer cations play an important role in enhancing ionic conductivity.

Figure 5 presents the plots of the logarithm of conductivity versus inverse temperature for LiV_3O_8, PMMA-(PC+DEC)-$LiClO_4$ and PMMA-LiV_3O_8-(PC+DEC)-$LiClO_4$ in the temperature range from 30 to 100 °C. The figure shows that the ionic conduction in nanocomposites polymer electrolytes obeys the Arrhenius relation

$$\sigma = \sigma_0 \exp(-E_a/kT) \tag{4}$$

where E_a is the activation energy, T is the temperature on Kelvin scale, σ_0 is the pre-exponential factor, and k is the Boltzmann constant. The activation energy for PMMA-LiV_3O_8 nanocomposite gel electrolyte is found to be 0.19 eV where as for pure LiV_3O_8 it is 0.25 eV. This decrease in activation energy in the nanocomposite could be attributed to the weaker columbic attraction of the layers to the Li^+ ions [39]. The decreased interaction between $V_3O_8^-$ layers and Li^+ ions is also corroborated by the FTIR results.

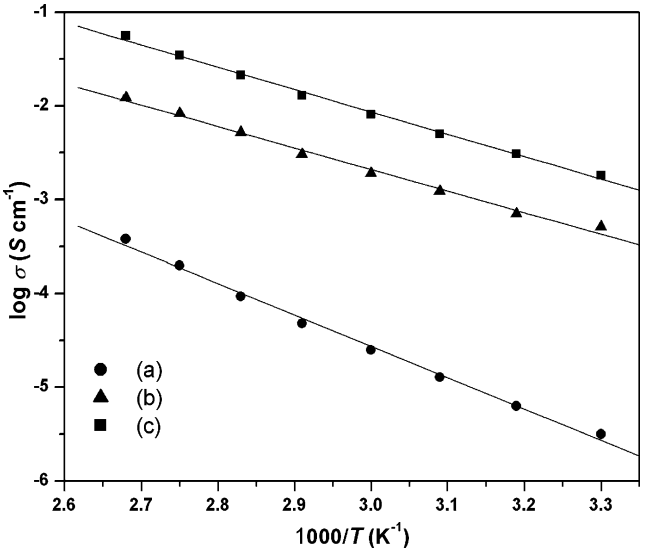

Fig. 5 log σ vs. temperature inverse curves for **a** LiV_3O_8, **b** PMMA-(PC+DEC)-$LiClO_4$ gel polymer electrolyte and **c** PMMA-LiV_3O_8-(PC+DEC)-$LiClO_4$ nanocomposite gel polymer electrolyte. Continuous solid lines represent fitting of experimental data by Arrhenius equation given by Eq. 4

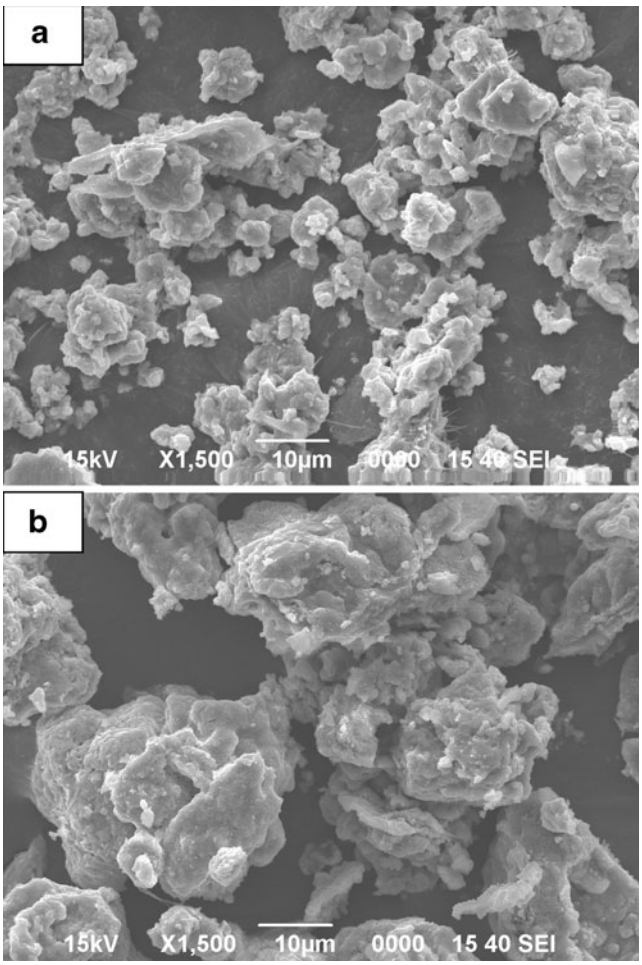

Fig. 6 Scanning electron micrographs of **a** pure LiV_3O_8 and **b** PMMA-LiV_3O_8 nanocomposite

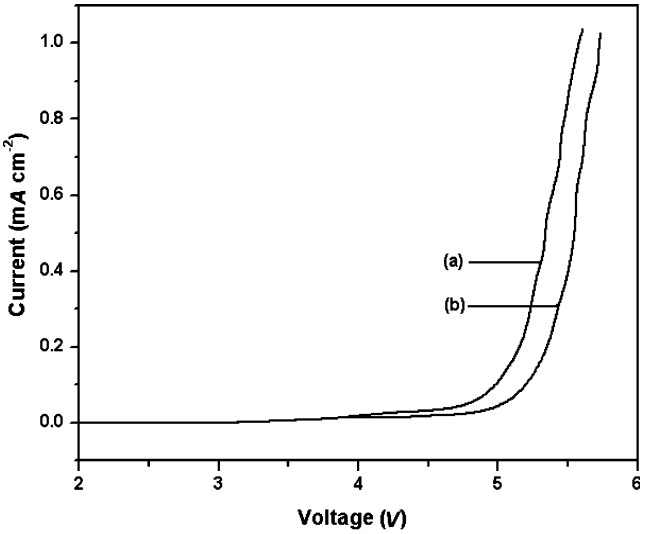

Fig. 7 Linear sweep voltammetry plots of **a** PMMA-(PC+DEC)-$LiClO_4$ gel electrolyte and **b** PMMA-LiV_3O_8-(PC+DEC)-$LiClO_4$ nanocomposite gel polymer electrolyte

Scanning electron microscopy studies

Scanning electron micrographs of pure LiV_3O_8 and PMMA-LiV_3O_8 nanocomposite are shown in Fig. 6a, b. It is observed from the Fig. 6a that LiV_3O_8 has particle size less than 8 μm (many of them are less than 3 μm). On the other hand SEM micrograph for PMMA-LiV_3O_8 exhibits aggregated particles having dimension greater than 20 μm (Fig. 6b). It is worth mentioning here that PMMA chains intercalate into the 6.3 Å channels of layered LiV_3O_8

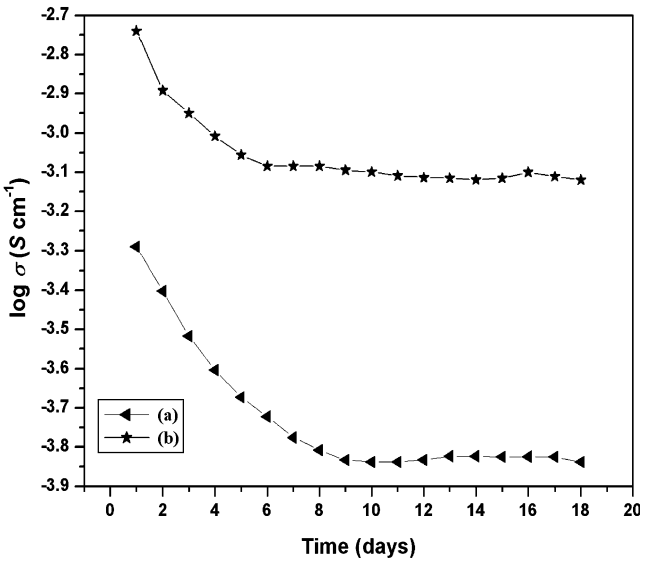

Fig. 8 Interfacial stability of **a** PMMA-(PC+DEC)-$LiClO_4$ gel electrolyte and **b** PMMA-LiV_3O_8-(PC+DEC)-$LiClO_4$ nanocomposite gel polymer electrolyte

increasing the interlayer spacing to 12.8 Å giving rise to nanoscale mixing of PMMA and LiV_3O_8 forming a PMMA-LiV_3O_8 nanocomposite, which is confirmed by XRD results. Aggregation of particles could be attributed to the fact that some PMMA chains extend from interlayer spacing of a LiV_3O_8 particle and intercalate into the interlayer spacing of the other LiV_3O_8 particle.

Electrochemical studies

Figure 7 displays the current-voltage response obtained for both PMMA-based gel polymer electrolyte and nanocomposite gel polymer electrolytes using stainless steel as a working electrode and lithium metal as a reference electrode measured between the potential ranges from 2 to 6 V with a scan rate 0.1 mVs^{-1}. The sudden rise of current identifies the anodic decomposition voltage of the electrolytes. It is observed that PMMA-based gel electrolyte shows decomposition voltage at 4.5 V whereas after intercalation value of decomposition voltage increases significantly and sets at about 4.8 V. Thus, there is a clear improvement in the voltage stability factor in the nanocomposite electrolyte. This value of working voltage range (i.e., electrochemical potential window) appears to be high enough to use the nanocomposite polymer electrolyte films as a solid-state separator/electrolyte in Li-batteries.

Compatibility of polymer electrolytes with electrode materials remains an acute problem for their application in high power lithium batteries. Due to the reactivity of electrode materials, most of the developed polymer electrolytes passivate lithium, which results in the formation of thick and non-uniform surface layer [40]. This can in turn encourage the formation and growth of lithium dendrites during charging period leading to internal short circuiting of the cell [41]. Therefore interfacial stability of polymer electrolytes in contact with electrode materials is an important factor for providing suitable performance in rechargeable lithium batteries. In order to examine the interfacial stability of PMMA-based gel polymer electrolyte and PMMA-LiV_3O_8-based nanocomposite gel polymer electrolyte, the ionic conductivity was measured by fabricating stainless steel/polymer electrolyte/stainless steel cells at room temperature and monitored for 18 days and their results are shown in Fig. 8. It reveals that ionic conductivity of both types of electrolytes decrease with time, but the decrease of ionic conductivity of PMMA-based gel polymer electrolyte is much larger as compared to that of PMMA-LiV_3O_8-based nanocomposite gel polymer electrolyte. Moreover the ionic conductivity of PMMA-LiV_3O_8-based nanocomposite gel polymer electrolyte becomes stable after 5 days whereas for PMMA-based gel polymer electrolyte ionic conductivity goes on decreasing up to 10 days. This confirms better interfacial stability of PMMA-LiV_3O_8-(PC+DEC)-$LiClO_4$ system over PMMA-(PC+DEC)-$LiClO_4$ system. It is well known that gel polymer electrolytes exhibit highly porous structure with interconnected pores to form continuous pathways between the cathode and the anode, thereby facilitating the formation and growth of lithium dendrites [8]. The porous structure of PMMA is disrupted in layered LiV_3O_8 which results in decrease in propagation of lithium dendrites leading to better interfacial stability than PMMA-based gel polymer electrolyte.

Conclusions

PMMA-LiV_3O_8 nanocomposite has been successfully synthesized using solution intercalation technique. The pellets obtained from synthesized nanocomposite have been dipped into liquid electrolytes containing 1 M $LiClO_4$ in PC/DEC (1:1 *v*/*v*) to synthesize PMMA-LiV_3O_8-(PC+DEC)-$LiClO_4$ nanocomposite gel polymer electrolyte. X-ray characterization indicates that the polymer chains are intercalated into the layers of LiV_3O_8. FTIR results indicate that the interaction between Li^+ ions and negative $V_3O_8^-$ layers is weakened due to increased interaction between Li^+ ions and inserted PMMA molecules. This provides a suitable two-dimensional path for Li^+ ion conduction. AC impedance analysis shows that nanocomposite gel polymer electrolyte exhibits room temperature ionic conductivity of 1.8×10^{-3} S cm^{-1}, which is about seven times larger than that for PMMA-(PC+DEC)-$LiClO_4$ electrolyte system. The enhancement in ionic conductivity is mainly attributed to the higher dielectric constant of layered host and aggregation of nanocomposites due to the extension of polymer chains from interlayer to the nanocomposite edge, which provides conduction paths for Li^+ ion transport. SEM results confirm the aggregation of nanocomposite particles. The interfacial stability of the nanocomposite gel polymer electrolyte is found to be better than the gel polymer electrolyte. The enhanced properties like higher ionic conductivity at ambient temperature and improved electrochemical properties make PMMA-LiV_3O_8-(PC+DEC)-$LiClO_4$ polymer electrolyte system particularly attractive for technological applications such as for rechargeable lithium batteries.

Acknowledgements The authors would like to thank Mr. Ratan Barua, Department of Physics, Tezpur University for extending help in taking SEM

References

1. Tarascon JM, Armand M (2001) Issues and challenges facing rechargeable lithium batteries. Nature (London) 414:359–367
2. Bertheir C, Gorecki W, Minier M, Armand MB, Chanbagno JM, Rigaud P (1983) Microscopic investigation of ionic conductivity

in alkali metal salts-poly(ethylene oxide) adducts. Solid State Ion 11:91–95
3. Nagasubramanian G, Attia AI, Halpert G (1994) A polyacrylonitrile-based gelled electrolyte: electrochemical kinetic studies. J Appl Electrochem 24:298–302
4. Morales E, Acosta JL (1997) Thermal and electrical characterization of plasticized polymer electrolytes based on polyethers and polyphosphazene blends. Solid State Ion 96:99–106
5. Abbrent S, Lindgren J, Tegenfeldt J, Wendsjo A (1998) Gel electrolytes prepared from oligo(ethylene glycol)dimethacrylate: glass transition, conductivity and Li^+-coordination. Electrochim Acta 43:1185–1191
6. Dolodnitsky D, Ardel G, Strauss E, Peled E, Lareah Y, Rigenberg Y (1997) Conduction mechanism in concentrated LiI-polyethylene oxide Al_2O_3-based solid electrolytes. J Electrochem Soc 144:3484–3491
7. Meyer WH (1998) Polymer electrolytes for lithium-ion batteries. Adv Mater 10:439–448
8. Song JY, Wang YY, Wan CC (1999) Review of gel-type polymer electrolytes for lithium-ion batteries. J Power Sources 77:183–197
9. Sekhon SS, Deepa M, Agnihotry SA (2000) Solvent effect on gel electrolytes containing lithium salts. Solid State Ion 136–137:1189–1192
10. Kim C-H, Lee K-H, Kim W-S, Park J, Seung D-Y (2001) Ion conductivities and interfacial characteristics of the plasticized polymer electrolytes based on poly(methyl methacrylate-co-Li maleate). J Power Sources 94:163–168
11. Svanberg C, Bergman R, Borjesson L, Jacobsson P (2001) Diffusion of solvent/salt and segmental relaxation in polymer gel electrolytes. Electrochim Acta 46:1447–1451
12. Vondrák J, Reitera J, Velická J, Sedlaříková M (2004) PMMA-based aprotic gel electrolytes. Solid State Ion 170:79–82
13. Sharma JP, Sekhon SS (2007) Nanodispersed polymer gel electrolytes: conductivity modification with the addition of PMMA and fumed silica. Solid State Ion 178:439–445
14. Rajendran S, Uma T (2000) Conductivity studies on PVC/PMMA polymer blend electrolyte. Mater Lett 44:242–247
15. Rajendran S, Kannan R, Mahendran O (2001) An electrochemical investigation on PMMA/PVdF blend-based polymer electrolytes. Mater Lett 49:172–179
16. Kumara R, Subramania A, Sundaram NTK, Vijaya Kumar G, Baskaran I (2007) Effect of MgO nanoparticles on ionic conductivity and electrochemical properties of nanocomposite polymer electrolyte. J Membr Sci 300:104–110
17. Ahmad S, Agnihotry AA, Ahmad S (2007) Nanocomposite polymer electrolytes by in situ polymerization of methyl methacrylate: for electrochemical applications. J Appl Polym Sci 107:3042–3048
18. Ruiz-Hitzky E (1994) Conducting polymers intercalated in layered solids. Adv Mater 5:334–340
19. Jeevanandam P, Vasudevan S (1998) Conductivity of a confined polymer electrolyte: lithium−polypropylene glycol intercalated in layered $CdPS_3$. J Phy Chem B 102:4753–4758
20. Arun N, Vasudevan S, Ramanathan KV (2000) Orientation and motion of interlamellar water: an infrared and NMR investigation of water in the galleries of layered $Cd_{0.75}PS_3K_{0.5}(H_2O)_y$. J Am Chem Soc 122:6028–6038
21. Chen H-W, Lin T-P, Chang F-C (2002) Ionic conductivity enhancement of the plasticized PMMA/$LiClO_4$ polymer nanocomposite electrolyte containing clay. Polymer 43:5281–5288
22. Singhal RG, Capracotta MD, Martin JD, Khan SA, Fedkiw PS (2004) Transport properties of hectorite based nanocomposite single ion conductors. J Power Sources 128:247–255
23. Maneghetti P, Qutubuddin S, Webber A (2004) Synthesis of polymer gel electrolyte with high molecular weight poly (methyl methacrylate)-clay nanocomposite. Electrochim Acta 49:4923–4931
24. de Picciotto LA, Adendorff KT, Liles DC, Thackeray MM (1993) Structural characterization of $Li_{1+x}V_3O_8$ insertion electrodes by single-crystal X-ray diffraction. Solid State Ionics 62:297–307
25. Liu Y-J, Schindler JL, DeGroot DC, Kannewurf CR, Hirpo W, Kanatzidis MG (1996) Synthesis, structure, and reactions of poly (ethylene oxide)/V_2O_5 intercalative nanocomposites. Chem Mater 8:525–534
26. Kanatzidis MG, Wu C-G, Mercy HO, Kannewurf C (1989) Conductive-polymer bronzes. Intercalated polyaniline in vanadium oxide xerogels. J Am Chem Soc 111:4139–4141
27. Jiao L, Li H, Yuan H, Wang Y (2008) Preparation of copper-doped LiV_3O_8 composite by a simple addition of the doping metal as cathode materials for lithium-ion batteries. Mater Lett 62:3937–3939
28. Ding Y, Gui Z, Zhu J, Hu Y, Wang Z (2009) Exfoliated poly (methyl methacrylate)/MgFe-layered double hydroxide nanocomposites with small inorganic loading and enhanced properties. Mater Res Bull 43:3212–3220
29. Li L, Yan Z (2005) Synthesis and characterization of self-assembled V_2O_5 mesostructures intercalated by polyaniline. J Nat Gas Chem 14:35–39
30. Pavia DL, Lampman GM, Kriz GS (2001) Introduction to spectroscopy, 3rd edn. Harcourt College Publ, USA
31. Kim CS, Oh SM (2000) Importance of donor number in determining solvating ability of polymers and transport properties in gel-type polymer electrolytes. Electrochim Acta 45:2101–2109
32. Rajendran S, Mahendran O, Kannan R (2002) Ionic conductivity studies in composite solid polymer electrolytes based on methylmethacrylate. J Phys Chem Solids 63:303–307
33. Yang G, Hou W, Sun Z, Yan Q (2005) A novel inorganic–organic polymer electrolyte with a high conductivity: insertion of poly (ethylene) oxide into LiV_3O_8 in one step. J Mater Chem 15:1369–1374
34. Saikia D, Kumar A (2005) Ionic transport in P(VDF-HFP)-PMMA-$LiCF_3SO_3$-(PC+DEC)-SiO_2 composite gel polymer electrolyte. Eur Polym J 41:563–568
35. de Picciotto LA, Adendorff KT, Liles DC, Thackeray MM (1993) Structural characterization of $Li_{1+x}V_3O_8$ insertion electrodes by single-crystal X-ray diffraction. Solid State Ion 62:297–307
36. Aravindan V, Vickraman P (2008) Characaterization of SiO_2 and Al_2O_3 incorporated PVdF-HFP based composite polymer electrolytes with $LiPF_3(CF_3CF_2)_3$. J Appl Polym Sci 108:1314
37. Appetecchi G, Croce F, Scrosati B (1995) Kinetics and stability of the lithium electrode in poly(methylmethacrylate)-based gel electrolytes. Electrochim Acta 40:991–997
38. Hayamizu K, Aihara Y, Arai S, Martinez CG (1999) Pulse-gradient spin-echo ^1H, ^7Li, and ^{19}F NMR diffusion and ionic conductivity measurements of 14 organic electrolytes containing $LiN(SO_2CF_3)_2$. J Phys Chem B 103:519–524
39. Manoratne CH, Rajapakse RMG, Dissanayake MAKL (2006) Ionic conductivity of poly(ethylene oxide) PEO-Montmorillonite (MMT) nanocomposited prepared by intercalation from aqueous medium. Int J Electrochem Sci 1:32–46
40. Croce F, Scrosati B (1993) Interfacial phenomena in polymer-electrolyte cells: lithium passivation and cycleability. J Power Sources 43:9–19
41. Stephan AM, Nahm KS, Kulandainathan MA, Ravi G, Wilson J (2006) Poly(vinylidene fluoride-hexafluoropropylene) (PVdF-HFP) based composite electrolytes for lithium batteries. Eur Polym J 42:1728–1734